Korean J. Chem. Eng., **31**(10), 1766-1772 (2014)
DOI: 10.1007/s11814-014-0078-3

pISSN: 0256-1115
eISSN: 1975-7220

Leaching kinetics of neodymium in sulfuric acid of rare earth elements (REE) slag concentrated by pyrometallurgy from magnetite ore

Ho-Sung Yoon*, Chul-Joo Kim*, Kyung Woo Chung*, Jin-Young Lee*, Shun Myung Shin*, Su-Jeong Lee, A-Ram Joe**, Se-Il Lee**, and Seung-Joon Yoo**,†**

*Korea Institute of Geoscience & Mineral Resources (KIGAM), 124, Gwahang-ro, Yuseong-gu, Daejeon 305-350, Korea
**Department of Environmental and Chemical Engineering, Seonam University,
7-111, Pyeongchon-gil, Songak, Asan 336-922, Korea
(*Received 11 January 2014 • accepted 7 March 2014*)

Abstract−We studied the leaching kinetics of recovering neodymium in sulfuric acid from the rare earth elements (REE) slag concentrated by smelting reduction from a magnetite ore containing monazite. The leaching kinetics on neodymium was conducted at a reactant concentration of 1.5 g REE slag per L of 0.3 M H_2SO_4, agitation of 750 rpm and temperature ranging from 30 to 80 ºC. Neodymium oxide included in the REE slag was completely converted into neodymium sulfate phase ($Nd_2(SO_4)_3$) in H_2SO_4 after the leaching of 5 h, 80 ºC. As a result, the leaching mechanism was determined in a two-stage model based on the shrinking core model with spherical particles. The first step was determined by chemical reaction, and the second step was determined by ash layer diffusion because the leaching of REEs by the first chemical reaction increases the formation of the ash layer affecting as a resistance against the leaching. By using the Arrhenius expression, the apparent activation energy of the first chemical reaction step was found to be 9 $kJmol^{-1}$. After the first chemical reaction, leaching reaction rate was determined by the ash layer diffusion. The apparent activation energy of ash layer diffusion was found to be 32 $kJmol^{-1}$.

Keywords: Leaching Kinetics, Magnetite Ore, Combinational Metallurgy, REE Slag, Neodymium Oxide, Neodymium Sulfate, Sulfuric Acid, Shrinking Core Model, Chemical Reaction, Ash Layer Diffusion

INTRODUCTION

Rare earth elements (REE) are a family of lanthanides ranging from lanthanum to lutetium, plus scandium and yttrium. They were named ìrare earth elementsî by IUPAC, but unlike the name, cerium is the 26th most abundant element, and neodymium is more abundant than gold in the earth's crust [1].

China provides 97% of the REE world's supply. While the demand is increasing in the field of leading edge industries such as fuel cells, mobile phones, displays, high-capacity batteries, permanent magnets for wind power, and green energy devices, China has recently done copious cuts of its export in the name of environmental protection. As the result, their supply has drastically diminished and the price of REEs has greatly increased.

Among the REEs, neodymium has been broadly used in various fields that require magnets with high magnetism, such as permanent magnets, cranking motor of automobiles, computers, audio-visual components, magnetic separators, and military and aerospace systems. The average annual growth in the magnet market has increased to 70% due to the increase in world demand over the last decade [2-5]. The price of neodymium recently skyrocketed from 14 US$/kg to 154 US$/kg, the highest increase rate of price among the REEs [6].

In the midst of world supply instability of REEs, the REE-free countries need to find an alternative solution to develop the new resources such as electronic-wastes (E-wastes) or low-grade ores. In the case of metallurgical method of these raw materials, there are two methods: pyrometallurgy and hydrometallurgy.

Generally, pyrometallurgy has been widely used in the treatment process of conventional high-grade ores to date, but the method is gradually losing its competitiveness in the treatment of low-grade ores due to the difficulty of treating small amounts, high energy consumption, many environmental pollutants and additional burdens on environmental treatment expense. Meanwhile, hydrometallurgy is an effective technology for the leaching of rare earths from low-grade metal resources because of the selective leaching by appropriate solvent, low process cost and occurrence of relatively little pollutants [7-15].

In this study, a combinational method using pyrometallurgy and hydrometallurgy is newly applied to attain the effective leaching of neodymium from magnetite ore [16-18].

THEORY

The leaching of REE slag is hypothesized by a shrinking core model with a constant size and a two-stage model with a chemical reaction and ash layer diffusion because REE slag is oxidized through the pyrometallurgy by arc furnace. Accordingly, the leaching mechanism assumes that the H_2SO_4 solution diffuses into ash layers remaining after the first chemical reaction. Finally, after the completion of leaching, REE slag only remains ash layers as shown in the leaching behavior diagram of Fig. 1.

†To whom correspondence should be addressed.
E-mail: sjyoo001@hanmail.net

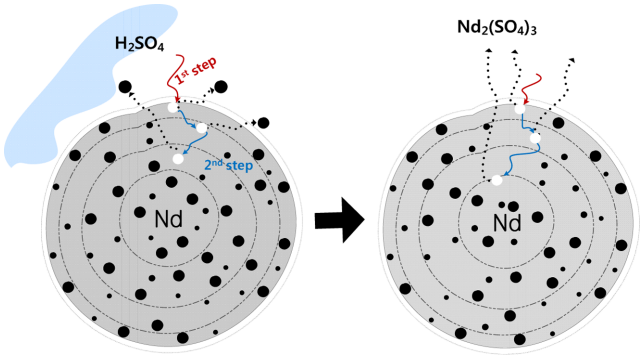

Fig. 1. Schematic diagram for the leaching behavior of neodymium from REE slag.

The Nd_2O_3 existing in the REE slag is converted into $Nd_2(SO_4)_3$ phase under H_2SO_4 solution as in the following Eq. (1).

$$3H_2SO_4(A)+Nd_2O_3(B)\rightarrow Nd_2(SO_4)_3+3H_2O \quad (1)$$

Assuming a first-order chemical reaction rate model based on the shrinking core model [19,20] with the same particle size before and after the leaching that has a spherical shape, the chemical reaction may be expressed in the following Eq. (2).

$$-\frac{1}{S_{ex}}\frac{dN_B}{dt}=-\frac{1/3}{4\pi r_c^2}\frac{dN_A}{dt}=-\rho_B\cdot\frac{dr_c}{dt}=\frac{1}{3}k_sC_A \quad (2)$$

However, the variation of can be ignored during the chemical reaction because the H_2SO_4 is added into the reactor excessively than the stoichiometric ratio. Since can be accepted as a constant in Eq. (2), this model is modified as follows:

$$1-(1-X_B)^{1/3}=k_{c,chem}t \quad (3)$$

The variation of H_2SO_4 (X_A) can be disregarded because it is excessively added. X_B is fractional conversion of neodymium in REE slag and $k_{c,chem}$ is the apparent rate constant for chemical reaction and inverse of the time required for complete conversion is given when r_c=0.

$$k_{c,chem}=\frac{C_{A0}k_s}{3\rho_B R} \quad (4)$$

R is the radius of initial REE slag particle. C_{Ao} is initial concentration of H_2SO_4. ρ_B is the molar density of neodymium in REE slag and k_s is the first-order rate constant for the chemical reaction.

During the chemical reaction, the neodymium oxide existing on the surface of REE slag is first leached out, and the ash layer remaining after the initial chemical reaction becomes thicker and acts as a resistance against the leaching reaction from the surface to inside core. Therefore, the ash layer diffusion can be considered as a second stage for the rate-determining step. In the ash layer diffusion model, there are many kinetic equations [21-23], but the reaction rate can be expressed in terms of the diffusion rate of H_2SO_4 through the ash layers by shrinking core model as follows:

$$1-3(1-X_B)^{2/3}+2(1-X_B)=k_{c,ash}t \quad (5)$$

$k_{c,ash}$ is the apparent rate constant for ash layer diffusion and inverse of the time required for complete conversion of a particle, r_c=0.

$$k_{c,ash}=\frac{2D_eC_{Ao}}{\rho_B R^2} \quad (6)$$

D_e is the effective diffusion coefficient of H_2SO_4 in the ash layer, R is the radius of initial REE slag particle. C_{Ao} is initial concentration of H_2SO_4. X_B is the fractional conversion of neodymium in REE slag and ρ_B is the molar density of neodymium in REE slag.

EXPERIMENTAL

1. Materials and Procedure

The raw material was magnetite ore containing monazite and collected from Hongcheongun in Korea. Monazite ($REEPO_4$) is primarily composed of rare earth phosphate, especially those of low atomic numbers such as Ce, La, and Nd along with the numerous other minor constituents such as Pr, Sm, and Gd etc. [24,25].

The magnetite ore contained 3% REEs, which was highly concentrated to 9% REEs in the slag after the separation of 55% iron by smelting reduction. At this time, 20 g silica as flux and 140 g coke as a reducing agent were added to 1 kg of ore, which was smelted in an arc furnace for two hours at 1,500 °C. 99% of the contained iron was extracted and 415 g of slag was recovered. The REE slag obtained after the smelting reduction process was milled and washed with water to remove impurities from the REE slag. Finally, the particle size had an average size of 100 μm. Rare earths in a magnetite ore were first concentrated into a slag phase by the pyrometallurgy of a reduction smelting process and then the REE slag was treated by hydrometallurgy as investigated in many researches [26-31].

The leaching experiment was carried out under the low slurry density of 1.5 g slag/L, 0.3 M H_2SO_4, with the agitation of 750 rpm at a temperature range of 30 to 80 °C using the Pyrex reactor volume of 1 L. The REE slag is composed of various REE oxide, polymetal silicate, and ash layers. A low slurry density was used to prevent gelation of dissolved silica during leaching. Mixing rate was fixed at high speed of 750 rpm to prevent yield reduction by low mixing rate.

2. Measurements

Metal compositions included in the REE slag were analyzed by inductively coupled plasma-mass spectrometry (ICP-MS, X-series (X5), Thermo Elemental, UK). ICP-MS was found to be the most suitable technique for the determination of REE content because it exhibits high sensitivity and accuracy, with high sample throughput. ICP-MS also allows rapid simultaneous multi-element determination [32].

The pH values were measured by pH electrode in advanced electrochemistry meter (Orion VERSASTAR, Thermo Scientific).

The morphologies of leach residues were observed by scanning electron microscope (15 kV, JEOL, JSM-6400). The samples for SEM investigation were prepared after the sufficient washing in water.

Sampled neodymium solution was filtrated by a syringe filter with 0.2 μm pores, and then neodymium ion concentration was analyzed by inductively coupled plasma-atomic emission spectrometry (ICP-AES, *i*CAP6000, Thermo Fisher, UK) during the leaching. At this time, the wavelength for ICP-AES analysis was selected at 430.3 nm, which is the condition to minimize interferences between the ele-

ments. When viscous silicate solution is injected into the plasma and nebulizer is blocked, the accuracy and detection limits of the ICP-AES are usually degraded. This problem could be avoided by limiting the input of viscous solution and by frequent washing of the nebulizer.

Nitrogen adsorption and desorption isotherms were measured for BET surfaces at 77 K using a Micromeritics TriStar 3000 automatic analyzer. Before the measurements, the samples were outgassed for 2 h in the degas port of the adsorption apparatus.

RESULTS AND DISCUSSION

As shown in Eh-pH diagram of Fig, 2, Nd_2O_3 is reduced into $Nd_2(SO_4)_3$ under the condition below the pH level of 4 at 30 °C and is precipitated by $Nd(OH)_3$ over the pH. Therefore, the leaching condition is desirable to keep the pH level below 4 for the sake of efficient leaching of neodymium. In this experiment, all the H_2SO_4 concentrations were fixed at 0.3 M to keep sufficient acidic solution condition below the pH level of 1.5.

Table 1 is an elemental composition of REE slag analyzed by ICP-MS. There are many chemical components in the REE slag. As shown in Table 1, 1.4% of neodymium component is included in the REE slag.

The neodymium was leached under a slurry density of 1.5 g slag/L H_2SO_4, with agitation at a temperature range of 30 to 80 °C. If metal components exist as the forms of the simple metal oxide, the stoichiometric ratio of H_2SO_4 (Merck, 98%) required to convert into sulfate forms is about 0.0018 M, but other REEs are simultaneously leached out in H_2SO_4 solution during the leaching period. Therefore, we added sulfuric acid of 0.3 M over the stoichiometric ratio reacting with all REEs in the slag, and kept the solution at a strong acidic condition of less than pH of 1.5.

As a result of N_2 adsorption and desorption, BET surface area had a value of 0.1 m^2/g before the leaching but 73.5 m^2/g after the leaching of 80 °C, 5 h as shown in Table 2. In the case of initial REE slag, N_2 gas was never adsorbed to REE slag because REE slag has no microstructure. On the other hand, in the case of REE slag after the leaching, it was converted from initial nonporous state to last

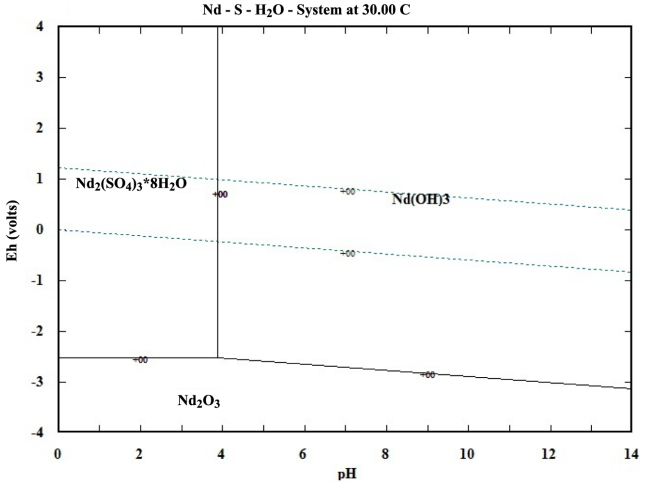

Fig. 2. Eh-pH diagram of neodymium chemical species in H_2SO_4 solution [33].

Table 1. Elemental composition of REE slag analyzed by ICP-MS

Element	Conc.	Element	Conc.	Element	Conc.
La	2.76%	Tb	24 ppm	U	2 ppm
Ce	4.60%	Dy	54 ppm	Fe	0.70%
Pr	0.41%	Ho	5 ppm	Ca	13.9%
Nd	1.14%	Er	17 ppm	Mg	7.10%
Sm	831 ppm	Tm	1 ppm	Ba	2.16%
Eu	159 ppm	Yb	9 ppm	Sr	9.84%
Gd	278 ppm	Lu	2 ppm	Y	122 ppm

Table 2. Physical properties of REE slag before and after leaching

Characteristic	Unit	Before leaching	After leaching
Surface area (BET)	m^2/g	0.1	73.5
Pore volume (BJH)	cm^3/g	Not detectable	0.26
Average pore size (BJH)	nm	Not detectable	14

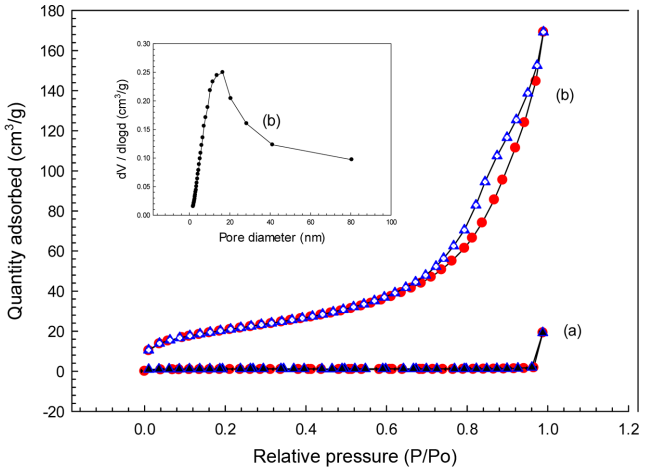

Fig. 3. N_2 gas adsorption and desorption isotherms of REE slag and pore size distribution before and after leaching; (a) before leaching (b) after leaching.

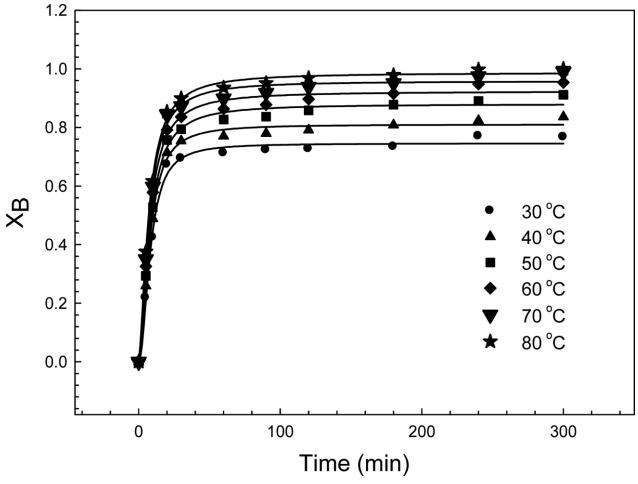

Fig. 4. Evolution of neodymium fractional conversion.

porous state because all the REEs leachable in H_2SO_4 solution were leached out during the leaching.

The N_2 adsorption-desorption isotherms of REE slag and pore size distribution before and after the leaching, are depicted in Fig. 3. Average pore size and pore volume were calculated by BJH method. On the other hand, for REE slag raw material we could not obtain pore size distribution data because it had no pores as expected. Pore size distribution and hysteresis were newly shown by pore formation during the leaching, and the average pore size was 14 nm and pore volume was 0.26 cm^3/g.

Fig. 4 represents the fractional conversion of neodymium during the leaching. As shown in Fig. 4, Nd_2O_3 existing in the REE slag was completely leached out to $Nd_2(SO_4)_3$ solution after the reaction of 5 h at the condition of 80 °C and 0.3 M H_2SO_4.

Many researchers have considered the leaching mechanism as single stage [34-55], two stages [56-58] or even three stages [59], but this study was applied to a two-stage model because the conversion rate of REE slag was divided into two stages, the first chemical reaction and the second ash layer diffusion on the basis of reaction time of 20 min as shown in Fig. 4.

Particle size of raw material had an average size of 100 μm, and it kept the same size after the leaching reaction as shown in Fig. 5.

BET surface area had a value of 0.1 m^2/g before the leaching but 73.5 m^2/g after the leaching of 80 °C, 5 h. This result conforms with the SEM result that REE slag is converted from nonporous state to porous state through the leaching.

Accordingly, the reaction introduced a shrinking core model with a constant particle size. The reaction rate was measured by analyzing the neodymium concentration by ICP-AES.

On the basis of the amount of REE components existing initially in the REE slag, the concentration of H_2SO_4 was added 0.3 M over the stoichiometric ratio of 0.0018 M H_2SO_4/1.5 g slag. Therefore, it was assumed that C_A is constant during the leaching.

The rate equation can be summarized as in Eq. (3) using the shrinking core model that has the shape of a spherical particle. On the basis of Eq. (3), the apparent rate constant ($k_{c,chem}$) can be calculated by the least square method at various reaction temperatures as shown in Fig. 6.

To examine the effect of reaction temperatures, the apparent activation energy was calculated from rate constants according to the temperatures as shown in Table 3. In the case of the chemical reaction control, the intercept was -1.064×10^3 as shown in Fig. 7. The apparent activation energy was determined to be 9 $kJmol^{-1}$ in the range of 30 to 80 °C. The small activation energy value shows that

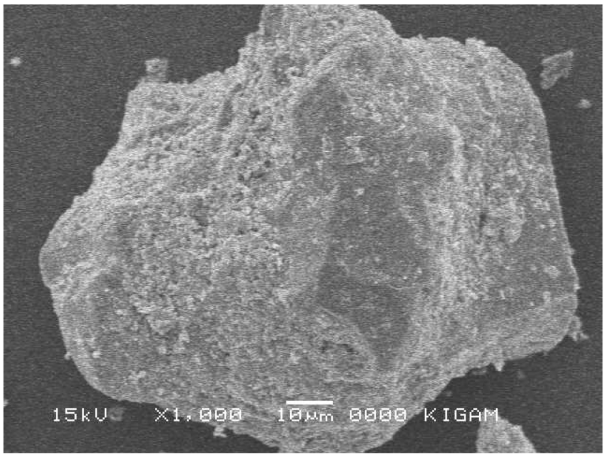

(a)

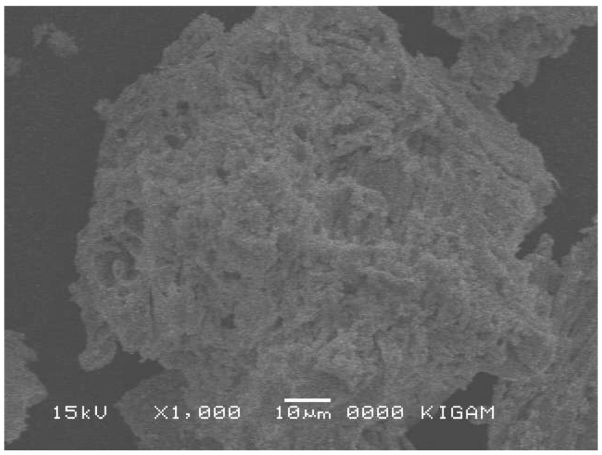

(b)

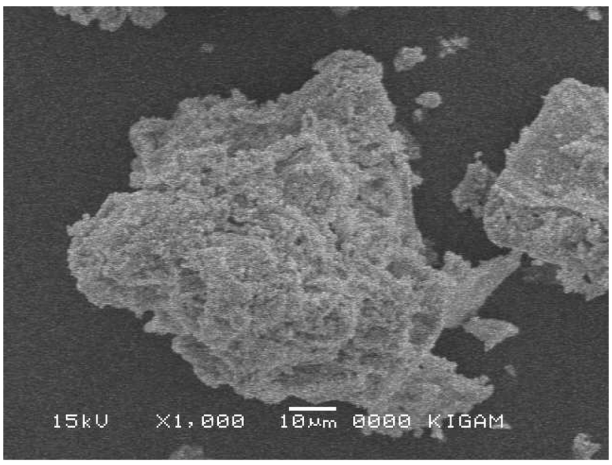

(c)

Fig. 5. SEM photographs of REE slag according to leaching times at 80 °C: (a) 0 min (b) 30 min (c) 300 min.

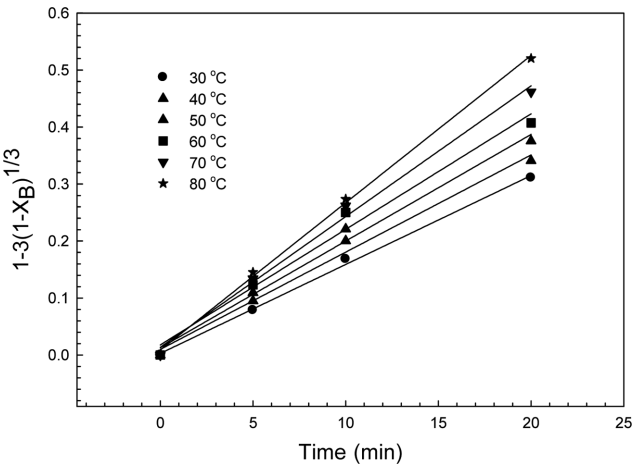

Fig. 6. Relationship between $1-3(1-X_B)^{1/3}$ and leaching times during the chemical reaction stage.

Table 3. Parameter searching data obtained from the regression for chemical reaction determining step

Parameter	30 °C	40 °C	50 °C	60 °C	70 °C	80 °C
a (slope)	1.560×10^{-2}	1.705×10^{-2}	1.871×10^{-2}	2.026×10^{-2}	2.293×10^{-2}	2.584×10^{-2}
b (y-intercept)	2.853×10^{-3}	9.933×10^{-3}	1.277×10^{-2}	1.783×10^{-2}	1.353×10^{-2}	8.822×10^{-3}
R^2	0.9978	1.0000	0.9903	0.9839	0.9941	0.9986

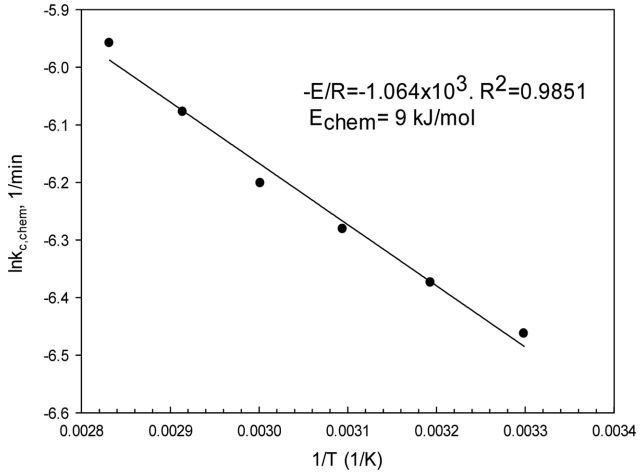

Fig. 7. Arrhenius plot of chemical reaction stage.

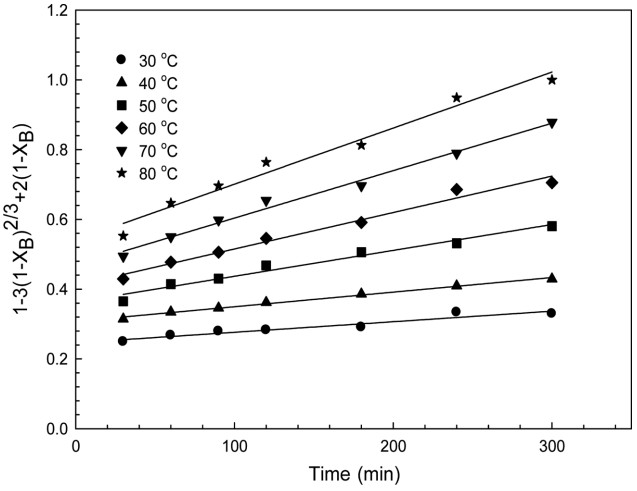

Fig. 8. Relationship between $1-3(1-X_B)^{2/3}+2(1-X_B)$ and leaching time during the ash layer diffusion stage.

this leaching reaction is insensitive to temperature change for the leaching of neodymium.

The chemical reaction is a rate determining step until 20 min. The slag surface becomes rough after the chemical reaction and only the ash layers remain. These ash layers will act as the resistance for H_2SO_4 to go into inner layers for the leaching. Accordingly, the ash layer diffusion was assumed as a second stage after the chemical reaction.

The rate equation can be summarized as in Eq. (5) for the ash layer diffusion rate-determining step using the shrinking core model that has the shape of a spherical particle. On the basis of Eq. (5), the apparent rate constant ($k_{c,ash}$) is calculated using the least square method at various reaction temperatures as shown in Fig. 8.

To investigate the effect of leaching temperatures, the apparent activation energy was calculated from rate constants shown in Table 4. In the ash layer diffusion stage, the slope was -3.830×10^3 as shown in Fig. 9. Finally, the apparent activation energy was found to be 32 $kJmol^{-1}$ in the temperature range of 30 to 80 °C.

This estimated activation energy is different from those values reported in the other ores. Feng et al. [60] studied the leaching kinetics of rare earth leaching from roasted ore of bastnaesite with sulfuric acid. It was found that the dissolution kinetics can be represented by shrinking-core model with diffusion through a product/ash layer diffusion as the rate-controlling step, and the activation energy was

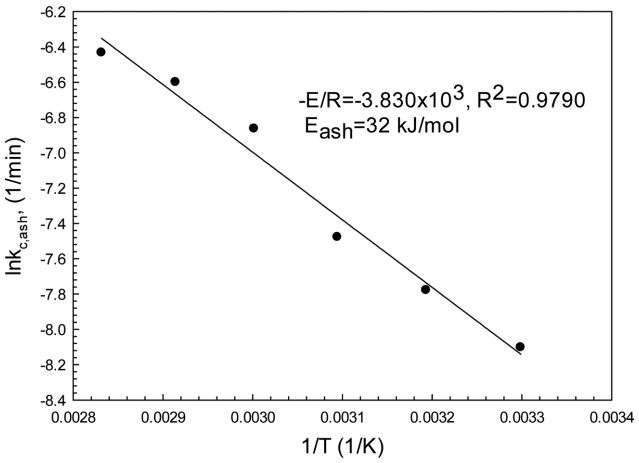

Fig. 9. Arrhenius plot of ash layer diffusion stage.

calculated to be 9.977 kJ/mol. Bian et al. [61] investigated the leaching kinetics of bastnaesite concentrate in HCl solution. It was found that the dissolution kinetics can be represented by shrinking-core model with diffusion through a product layer as the rate-controlling step, and the activation energies for $RE_2(CO_3)$ and REF_3 leached

Table 4. Parameter searching data obtained from the regression for ash layer diffusion determining step

Parameter	30 °C	40 °C	50 °C	60 °C	70 °C	80 °C
a (slope)	3.026×10^{-4}	4.186×10^{-4}	5.651×10^{-4}	1.045×10^{-3}	1.360×10^{-3}	1.607×10^{-3}
b (y-intercept)	2.461×10^{-1}	3.077×10^{-1}	4.635×10^{-1}	4.107×10^{-1}	4.678×10^{-1}	5.403×10^{-1}
R^2	0.9230	0.9923	0.9892	0.9804	0.9899	0.9755

from bastnaesite concentrate were calculated to be 59.39 kJ/mol and 66.13 kJ/mol, respectively.

The difference in activation energies is probably due to the existence of different neodymium compounds in the raw material.

In this experiment, silica was added as a flux to increase fluid flow of raw material in the pyrometallurgical process. As a result, the silica brought about the formation of complex polymetal oxide compounds. These compounds were induced the gelation by formation of silicate during the hydrometallurgy and complex leaching behaviors.

CONCLUSIONS

This study was carried out using the combinational method of hydrometallurgy and pyrometallurgy for the leaching of effective neodymium from a low grade Hongcheon magnetite ore. The magnetite ore was first concentrated to 9% REEs in the slag by pyrometallurgy of 1,500 °C after the dressing treatment and then it was used as a raw material for hydrometallurgy.

Leaching reaction mechanism was proposed by a two-stage shrinking core model as a leaching mechanism of neodymium oxide in the H_2SO_4 from REE slag.

The first reaction was determined by chemical reaction and the second reaction was determined by ash layer diffusion.

1. REE slag was converted from initial nonporous state of 0.1 m^2/g to final porous state of 73.5 m^2/g after the leaching because REEs were leached out during the leaching. Thus effective leaching was performed in this experimental condition.

2. The first reaction was rapidly leached out by chemical reaction for 20 min. The reaction rate and yield increased with increasing temperatures. In the first chemical reaction stage, the activation energy was found to be 9 $kJmol^{-1}$ in the temperature range of 30 to 80 °C. The postulated reaction was well conformed both by the linear relationship of the rate constant and the apparent activation energy.

3. In the second ash layer diffusion stage, the apparent activation energy was found to be 32 $kJmol^{-1}$, which is larger than the chemical reaction. Therefore, temperature dependence in the ash layer diffusion stage was more temperature-sensitive than the chemical reaction stage.

ACKNOWLEDGEMENT

The research was supported by the Basic Research Project of Korea Institute of Geoscience and Mineral Resources (KIGAM) funded by the Minister of Science, ICT and Future planning of South Korea.

NOMENCLATURE

C_A : concentration of H_2SO_4 reactant [$molL^{-1}$]
C_{A0} : initial concentration of H_2SO_4 reactant [$molL^{-1}$]
C_B : concentration of REE slag reactant [$molL^{-1}$]
C_{B0} : initial concentration of REE slag reactant [$molL^{-1}$]
E_{Chem} : apparent activation energy for chemical reaction [$kJmol^{-1}$]
E_{Ash} : apparent activation energy for ash layer diffusion [$kJmol^{-1}$]
k_s : first-order rate constant for the chemical reaction [s^{-1}]
$k_{c,\,chem}$: apparent rate constant for chemical reaction [s^{-1}]
$k_{c,\,ash}$: apparent rate constant for ash layer diffusion [s^{-1}]
N_A : moles of H_2SO_4 reactant [mol]
N_B : moles of REE slag reactant [mol]
N_{B0} : initial moles of REE slag reactant [mol]
r_c : radius of unreacted slag [m]
R : radius of initial slag [m]
S_{ex} : external surface area [m^2]
t : time [s]
T : temperature [K]
X_A : fraction of converted H_2SO_4
X_B : fraction of converted neodymium in REE slag

Greek Letter

ρ_B : molar density of neodymium component included in slag [$molL^{-1}$]

REFERENCES

1. S. Massari and M. Ruberti, *Resources Policy*, **38**, 36 (2013).
2. C. Jirang and Z. Lifeng, *J. Hazard. Mater.*, **158**, 228 (2008).
3. J.-C. Lee, H. T. Song and J.-M. Yoo, *Conservation and Recycling*, **50**, 380 (2007).
4. A. Tuncuk, V. Stazi, A. Akcil, E. Y. Yazici and H. Deveci, *Miner. Eng.*, **25**, 28 (2012).
5. I. C. Nnorom and O. Osibanjo, *Conservation and Recycling*, **52**, 843 (2008).
6. M. Stefania and R. Marcello, *Resources Policy*, **3**, 36 (2013).
7. M. Aarabi-Karasgani, F. Rashchi, N. Mostoufi and E. Vahidi, *Hydrometallurgy*, **102**, 14 (2010).
8. R. Dehghan, M. Noaparast and M. Kolahdoozan, *Hydrometallurgy*, **96**, 275 (2009).
9. Y. A. El-Nadi, *Hydrometallurgy*, **119**, 23 (2012).
10. M. Kul, Y. Topkaya and I. Karakaya, *Hydrometallurgy*, **93**, 129 (2008).
11. K. Liu, Q. Chen, Z. Yin, H. Hu and Z. Ding, *Hydrometallurgy*, **125**, 125 (2012).
12. L. Minting, W. Chang, Q. Shuang, Z. Xuejiao, L. Cunxiong and D. Zhigan, *Hydrometallurgy*, **104**, 193 (2010).
13. G. A. Moldoveanu and V. G. Papangelakis, *Hydrometallurgy*, **117**, 71 (2012).
14. S.-J. Yoo, H. S. Yoon, H. D. Jang, M.-J. Lee, S.-I. Lee, S.-T. Hong and H. S. Park, *Chem. Eng. J.*, **133**, 79 (2007).
15. S.-J. Yoo, D.-H. Kwak, J.-W. Lee, U.-Y. Hwang and H.-D. Jang, *Hydrometallurgy*, **96**, 223 (2009).
16. J. R. Dodson, A. J. Hunt, H. L. Parker, Y. Yang and J. H. Clark, *Chem. Eng. Process.*, **51**, 69 (2012).
17. I. Kostova, *Curr. Med. Chem.* **5**, 591 (2005).
18. A. J. Manhique, W. W. Focke and M. Carvalho, *Hydrometallurgy*, **109**, 230 (2011).
19. O. Levenspiel, *Chemical Reaction Engineering*, 3rd Ed., John Wiley & Sons Inc., New York (2003).
20. L. D. Schmidt, *The Engineering of Chemical Reactions*, 2nd Ed., Oxford University Press (2005).
21. M. Avrami, *J. Chem. Phys.*, **7**, 1103 (1939).
22. C. F. Dickinson and G. R. Heal, *Thermochim. Acta*, **340**, 89 (1999).
23. J. J. M. Órfão and F. G. Martins, *Thermochim. Acta*, **390**, 195 (2002).
24. Y. Kanazawa and M. Kamitani, *J. Alloys Compd.*, **408**, 1339 (2006).
25. Y. A. El-Nadi, J. A. Daoud and H. F. Aly, *Int. J. Miner. Process*, **76**,

101 (2005).
26. Y. Ding, Q. Xue, G. Wang and J. Wang, *Matallurgy and Materials Transactions B*, **28**, 28 (2013).
27. A. Fozia, S. Muhammad and A. Ata, *Hydrometallurgy*, **117**, 1 (2012).
28. A. M. Georgiana and G. P. Vladimiros, *Hydrometallurgy*, **117**, 71 (2012).
29. A. T. Kandil, M. M. Aly, E. M. Moussa, A. M. Kamel, M. M. Gouda and M. N. Kouraim, *J. Rare Earths*, **28**, 576 (2010).
30. D. J. Sapsford, R. J. Bowell, J. N. Geroni, K. M. Penman and M. Dey, *Miner. Eng.*, **39**, 165 (2012).
31. J. Tian, J. Yin, R. Chi, G. Rao, M. Jiang and K. Ouyang, *Hydrometallurgy*, **101**, 166 (2010).
32. T. N. Akinlua and T. R. Ajayi, *Fuel*, **87**, 1469 (2008).
33. HSC Chemistry 5.0 Chemical Reaction and Equilibrium Software with Extensive Thermochemical Database, Ver 5.11, Outokumpu Research, Finland.
34. M. Gharabaghi, M. Noaparast and M. Irannajad, *Hydrommetallurgy*, **95**, 341 (2009).
35. Y. Kadioglu, S. Karaca and S. Bayrakceken, *Fuel Process. Technol.*, **41**, 273 (1995).
36. F. W. Y. Momade and Z. G. Momade, *Hydrometallurgy*, **54**, 25 (1999).
37. H. Okur, T. Tekin, A. K. Ozer and M. Bayramoglu, *Hydrometallurgy*, **67**, 79 (2002).
38. M. Alkan and M. Dogan, *Chem. Eng. Process.*, **43**, 867 (2004).
39. O. Lacin, B. Donmez and F. Demir, *Int. J. Miner. Process.*, **75**, 91 (2005).
40. F. Bakan, O. Lacin, B. Bayrak and H. Sarac, *Int. J. Miner. Process.*, **80**, 27 (2006).
41. S. Aydogan, M. Erdemoglu, A. Aras, G. Ucar and A. Ozkan, *Hydrometallurgy*, **84**, 239 (2006).
42. A. D. Souza, P. S. Pina, E. V. O. Lima, C. A. Da Silva and V. A. Leao, *Hydrometallurgy*, **89**, 337 (2007).
43. A. Ekmekyapar, N. Demirkiran and A. Kunkul, *Chem. Eng. Res. Des.*, **86**, 1011 (2008).
44. A. D. Souza, P. S. Pina, F. M. F. Santos, C. A. Da Silva and V. A. Leao, *Hydrometallurgy*, **95**, 207 (2009).
45. B. Donmez, F. Demir and O. Lacin, *J. Ind. Eng. Chem.*, **15**, 865 (2009).
46. M. S. Safarzadeh, D. Moradkhani and M. Ojaghi-Ilkhchi, *J. Hazard. Mater.*, **163**, 880 (2009).
47. T. Heydarpour, B. Rezai and M. Gharabaghi, *Chem. Eng. Res. Des.*, **89**, 2153 (2011).
48. A. T. Kandi, M. M. Aly, E. M. Moussa, A. M. Kamel, M. M. Gouda and M. N. Kouraim, *J. Rare Earths*, **28**, 576 (2010).
49. R. Guliyev, S. Kuslu, T. Calban and S. Colak, *J. Ind. Eng. Chem.*, **18**, 1202 (2012).
50. M. Gharabaghi, M. Irannajad and A. R. Azadmehr, *Sep. Purif. Technol.*, **86**, 9 (2012).
51. P. Raschman and E. Smincakova, *Hydrometallurgy*, **113**, 60 (2012).
52. H. Huang, J. Li, X. Li and Z. Zhang, *Sep. Purif. Technol.*, **108**, 45 (2013).
53. D. Gaoxiang, L. Guocheng and H. Zuwen, *Chin. J. Chem. Eng.*, **21**, 736 (2013).
54. M. Gharabaghi, M. Irannajad and A. R. Azadmehr, *Chem. Eng. Res. Des.*, **91**, 325 (2013).
55. X. Feng, Z. Long, D. Cui, L. Wang, X. Huang and G. Zhang, *Tran. Nonferrous Met. Soc. China*, **23**, 849 (2013).
56. J. P. Martins, *Hydrometallurgy*, **42**, 221 (1996).
57. A. D. Souza, P. S. Pina, V. A. Leao, C. A. Silva and P. F. Siqueira, *Hydrometallurgy*, **89**, 72 (2007).
58. M. Aarabi-Karasgani, F. Rashchi, N. Mostoufi and E. Vahidi, *Hydrometallurgy*, **102**, 14 (2010).
59. K. Liu, Q. Chen, Z. Yin, H. Hu and Z. Ding, *Hydrometallurgy*, **125**, 125 (2012).
60. X. Feng, Z. Long, D. Cui, L. Wang, X. Huang and G. Zhang, *Trans. Nonferrous Met. Soc. China*, **23**, 849 (2013).
61. X. Bian, S. Yin, Y. Luo and W. Wu, *Trans. Nonferrous Met. Soc. China*, **21**, 2306 (2011).